



Behavior of High Strength Hybrid Reinforcement Concrete Beams

Khanda Ali Al-Billbassi^{1*}, Dr. Mushriq Fuad Kadhim Al-Shamaa¹

¹Department of Civil Engineering, College of Engineering,
University of Baghdad, Baghdad, Al-Jadriya, IRAQ

*Corresponding Author

DOI: <https://doi.org/10.30880/ijie.2020.12.07.028>

Received 3 September 2020; Accepted 12 October 2020; Available online 31 October 2020

Abstract: Six proposed simply supported high strength-steel fiber reinforced concrete (HS-SFRC) beams reinforced with FRP (fiber reinforced polymer) rebars were numerically tested by finite element method using ABAQUS software to investigate their behavior under the flexural failure. The beams were divided into two groups depending on their cross sectional shape. Group A consisted of four trapezoidal beams with dimensions of (height 200 mm, top width 250 mm, and bottom width 125 mm), while group B consisted of two rectangular beams with dimensions of (125 × 200) mm. All specimens have same total length of 1500 mm, and they were also considered to be made of same high strength concrete designed material with 1% volume fraction of steel fiber. Different types and ratios of FRP rebar were used to reinforce these test beams. The study's principle variables were the amount and type of flexural reinforcement (glass FRP and basalt FRP) and beam cross-sectional shape (rectangular and trapezoidal). The load-deflection behavior and ultimate load capacity of the beams were studied and compared with one another under flexural test with symmetrical two-point loading. The results show that increasing the reinforcement ratio resulted in higher post cracking flexural stiffness, and higher residual strength, as well as caused an increase in the first cracking load and ultimate load capacity ranged from 3 to 16.9%, and 4.6 to 7.3% respectively. When the GFRP rebars replaced by BFRP, the overall beams flexural performance showed outstanding improvements. Moreover the results indicate that increasing the top width of the beam cross section led to a significant enhancement in the first crack load ranged from 16 to 32.4%, also a remarkable increases in the ultimate load capacity in the range of 35.5 to 35.8% were indicated in the trapezoidal beams compared to rectangular beams. However the results show that the deflections were similar and were approximately 1.07–1.54 mm for all test beams. It is worth noting that the general flexural behavior of all the test beams indicated a ductile behavior with a gradual reduction in strength and high residual strength pre to failure due to proposing steel fiber presence.

Keywords: Steel fiber, Trapezoidal cross section, High strength concrete beams, FRP bars, Finite element method, ABAQUS software, Flexural behavior

1. Introduction

Due to the brittle nature of concrete material, especially high strength concrete (HSC) type [1], and the linear elastic behavior of fiber reinforced polymer (FRP) rebar, which results in no ductility response in the flexural behavior of FRP reinforced beams in comparison with the steel reinforced structures [2]. The use of concrete beams reinforced by FRP materials requires ductility modifications of the concrete structural elements, therefore, over the years a great deal of efforts has been made to define and enhance FRP bar-reinforced beams ductile behavior.

So far, the research scientists introduced three approaches. One approach is to use hybrid FRP rebar, which is defined as materials with pseudo-ductile and fabricated by combining more than one type of FRP reinforcing materials to present

a simulation of the elastic-plastic behavior of the steel reinforced bars. Belarbi, Chandrashekhara and Watkins [3], and Harris, Somboonsong, and Ko [4] conducted tests on beams reinforced with hybrid-FRP rebars and they reported that the ductile behavior of those beams could be close to that of steel reinforced beams. Despite the success of this method in research fields, but has encountered limitations in term of practical applications due to the complicated and costly manufacturing process of the hybrid FRP rebars.

The other approach is to use hybrid reinforcement (steel + FRP rebar) by partially replace the amount required of steel reinforcement to reinforce a beam with FRP rebars as conducted by Seongeun, and Seunghun [5]. Studies and tests were carried out by Yinghao, and Yong [6] on the flexural behavior of normal and HSC beams reinforced with hybrid reinforcements (steel + GFRP rebars) as a step toward decreasing of the non-ductile performance of mono reinforcement type of FRP reinforced beams. However, despite the success of this method in significantly increasing the ductility of the system but still not to be considered when the main goal is to eradicate the problems related to steel reinforcement corrosion since the presence of steel rebars is still there.

Another approach which is considered as the most important one conducted to this day, is to ameliorate the property of concrete i.e. defining the systems ductility is strongly dependent on the concrete properties. ACI 440.1R-15 [7] recommends over-reinforcing the FRP reinforced structures and designing the beams to fail by concrete crushing rather than by FRP rebar rupture. However, the most focus was on the employ of steel fibers, for several reasons including having high tensile strength and proven to have the ability to bridge cracks and narrowing the crack width [8–9]. Such characteristics of steel fiber can be employed to change the brittle performance of concrete under tensile stresses to a more ductile performance. Alsayed and Alhozaimy [10] reported that with the 1% addition of steel fibers, the ductility index increased by as much as 100%.

In this study another approach was discussed for the flexural behavior of FRP bar-reinforced concrete beams, which is utilizing HS concrete material with steel fiber addition combined with a trapezoidal cross section by increasing the top width, thus increasing the compression area, which has been proven by Shafeeq, Al-Shathr, and Al-Hussnawi [11] to result in higher ultimate load capacity and lower deflection. The different behaviors of HS-SFRC beams with different type and amount of FRP reinforced bars are also discussed.

2. Objectives

The main objective of this study is to develop a non-ferrous hybrid reinforcing system for concrete beams by employing continuous FRP reinforced bars incorporated with short discontinuous randomly distributed steel fiber, as well as utilizing a trapezoidal cross-section. This hybrid system has the potential to terminate problems related to steel reinforcement corrosion, while providing required strength, stiffness, and coveted ductility, which are drawbacks associated with conventional concrete structures constructed with FRP reinforcement system.

3. Proposed Beam Models Details

A total of six simply supported HS-SFRC beams proposed models were numerically tested in this research. These test beams are divided into two groups depending on their cross section shape. Group A consist of four trapezoidal cross section beams with dimensions of (bottom width of 125mm, top width of 250 mm, and total height of 200 mm), while Group B consist of two rectangular beam with proposed dimensions of (125×200) mm. All beams have same total length of 1500 mm, and they are supposed to be contained 1% of steel fiber having length of 35 mm and aspect ratio of 64. The proposed compressive strength f'_c was 60 MPa for all test beams. Different types and diameters of FRP (GFRP, and BFRP) rebars (Fig. 8), were used to reinforce these proposed beams in tension zone. More details of the flexural reinforcement for each test beam are shown in Table (1). Moreover, these beams are analytically subjected to two concentrated loads up to failure with a distance of 260 mm between them at the center of the beams leaving 520 mm of shear span at each side. To avoid shear failure, sufficient amount of steel stirrups with diameter of 8 mm were used in all models within the shear span. Two nominal of 8 mm steel bars were used as top reinforcement to hold the stirrups. To prevent local failure, steel plates of dimensions (250×100×25) mm are proposed to be located under the applied loads, while steel plates with dimensions (125×100×25) mm are located at the support at each side and contacted to the model bottom side face.

Fig. 1 shows the nomenclature of the tested beams, while Table 1 describes the proposed beams designations and details.

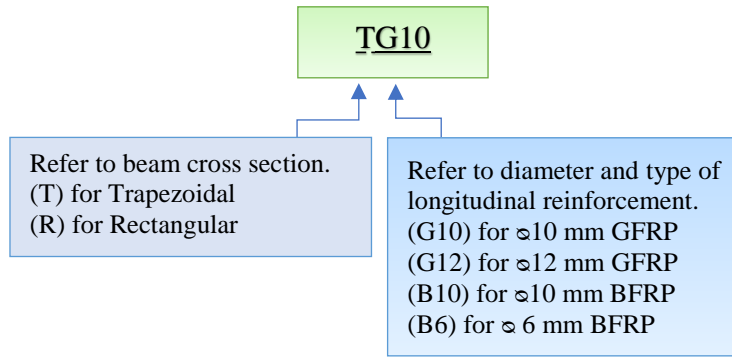


Fig. 1 - Nomenclature of the tested beams

Table 1 - Details of proposed beams

Group design	Beam designation	Steel fiber	Main rebar details	Main rebar type	Total length
A	TG10	1%	2 ϕ10 mm	GFRP	1500 mm
	TG12	1%	2 ϕ12 mm	GFRP	1500 mm
	TB10	1%	2 ϕ10 mm	BFRP	1500 mm
	TB6	1%	2 ϕ6 mm	BFRP	1500 mm
B	RG10	1%	2 ϕ10 mm	GFRP	1500 mm
	RB6	1%	2 ϕ6 mm	BFRP	1500 mm

4. Finite Element Modeling

The two proposed groups of HS-SFRC simply supported beams, which have been detailed in the above sections, are executed in the finite element analysis (FEA) employing ABAQUS computer program.

4.1 Discretization of The Beams

HS-SFRC beams reinforced with FRP reinforcement are discretized and analyzed using 8-noded reduced integration linear brick hourglass control elements (C3D8R) with 3-degree of freedom for concrete as well as for both loading and supporting plates. Two-noded three-dimensional linear truss elements (T3D2) were used to simulate the FRP flexural rebars, and steel stirrups as well as top reinforcing steel bars (stirrup-holders).

To model solid 3D element, C3D8 can be applied as it has the capability of interpreting the tension cracking in concrete, and the concrete crushing in compression, as well as the depiction of creep and large strain.

For reinforcing bars modeling, T3D2 element is used, as it considers the stretching of the bars in axial direction only.

The interaction between the concrete and both FRP bars and steel stirrups simulated via applying the constraint function of embedded region i.e. interpreting FRP rebars and steel stirrups to be embedded in concrete [12, 13] taking into consideration the perfect bond between the reinforcing bars (FRP, and stirrups) and the HS-SFRC, which means same nodes are shared by the two materials via using the link element. This type of interaction of embedded region with perfect bond is also applied between the HS-SFRC and the stirrups.

To model the loading and supporting steel plates, tied constrain surface to surface interaction was considered between the concrete and these plates with a master-slave (steel-concrete) contact. The material of steel plates were modeled as made of ideal-elastic material i.e. defining only Young's modulus by 200 GPa and Poisson's ratio by 0.3. For boundary conditions to be modeled in ABAQUS, displacement rotation conditions were required to constraint the model to get a characteristic solution. The partition tool was used to create a center line support at each supporting plate. The support was simulated as simple hinge and roller supports by restraining appropriate degrees of freedom at nodes on the corresponding positions (supporting plates). Static loading was achieved by defining two reference points at the top of loading plates and assigning prescribed displacement with different rates to these points. Figures 3 and 4 show the layout details and finite element modeling of the proposed beams.

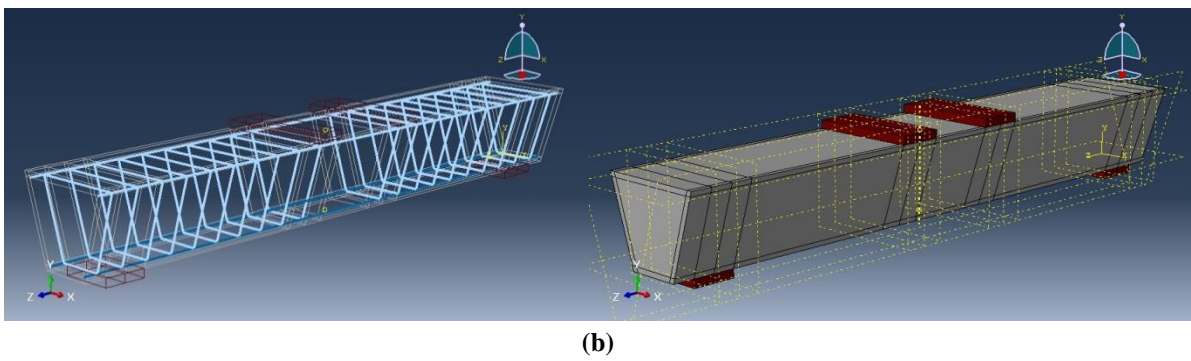
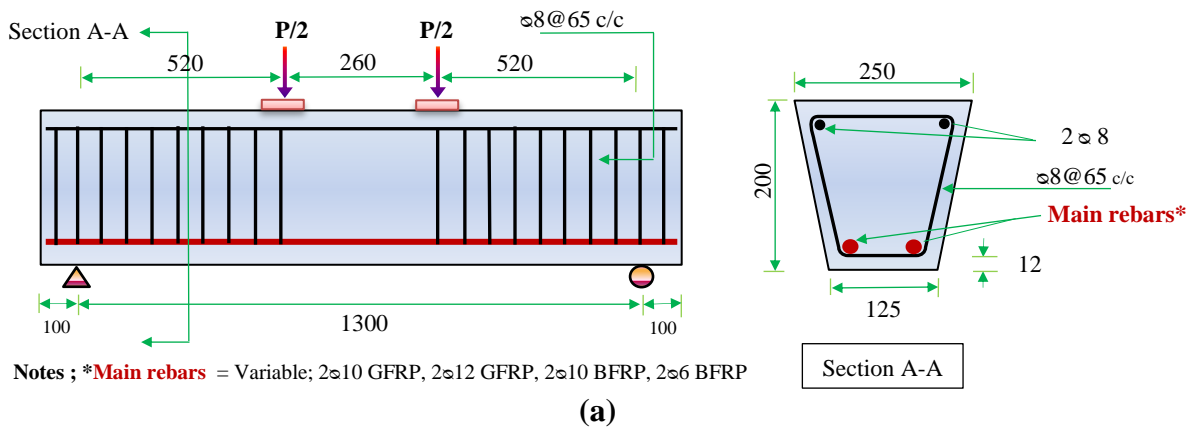


Fig. 3 - The proposed trapezoidal beams; (a) Layout details (dimensions are mm); (b) Finite element modeling

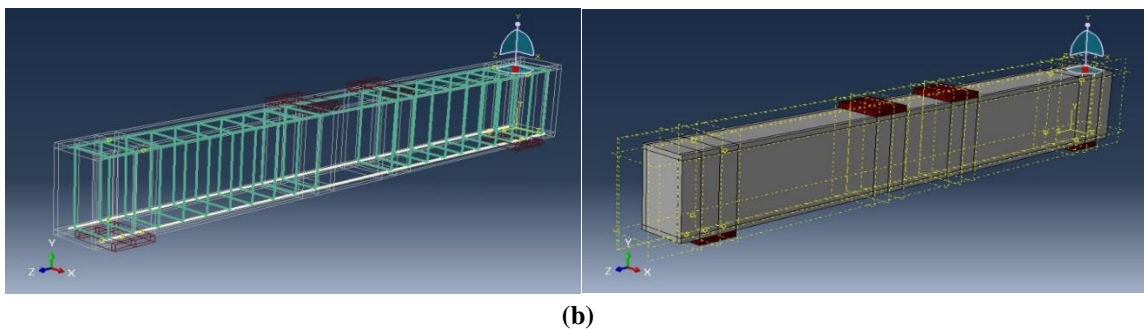
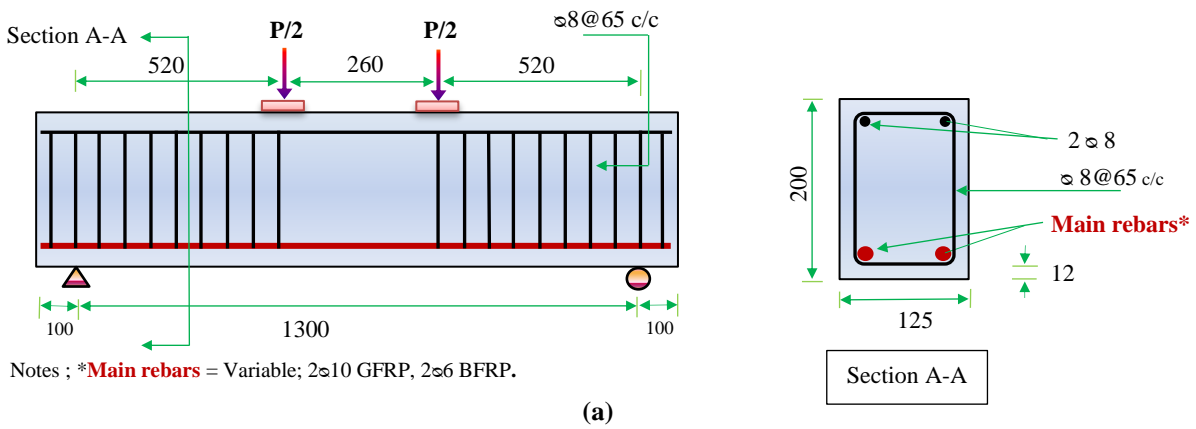


Fig. 4 - The proposed rectangular beams; (a) Layout details (dimensions are mm); (b) Finite element modeling

4.2 Material Modeling

4.2.1 Modeling of Steel Fiber Reinforced Concrete

ABAQUS concrete plasticity model (damage based), is utilized to depict the nonlinearity behavior of HS-SFRC material. The model of concrete damage plasticity (CDP) adopt the assumption of isotropic damage transformation. This adoption is merged with isotropic tensile and compressive plasticity to imitate the inelastic phase of the concrete behavior. In order for the analysis to transpire, CDP model definition shall be specified through a set of material properties as outlined below.

- **Stress-strain curve in compression**

There are two methods to model the materials of SFRC of the proposed beams. The first method is to take the effect of steel fiber on the mechanic properties of concrete into consideration, the other method is to neglect that effect and the steel fiber is modeled as smeared reinforcement [14]. In this study the first method is considered to model the steel fibrous concrete. Therefore the equation proposed by Carreira and Chu [15], Eq. 1 was chosen to represent the uniaxial compression stress-strain curve with nonlinear regressions conducted and validated by Júnior and Borges [16] of curves formed similar to experimental curves for obtaining the value of the parameter β via Eq. 2, also for estimating the peak strain $\varepsilon_{c,o}$ via Eq. 3.

$$\frac{\sigma_c}{f_c} = \frac{\beta \left(\frac{\varepsilon_c}{\varepsilon_{c,o}} \right)}{\beta - 1 + \left(\frac{\varepsilon_c}{\varepsilon_{c,o}} \right)^\beta} \quad (1)$$

$$\beta = (0.0536 - 0.5754 \mathcal{V}_f) f_c \quad (2)$$

$$\varepsilon_{c,o} = (0.00048 + 0.01886 \mathcal{V}_f) \ln f_c \quad (3)$$

Where σ_c and f_c are compressive stress and compressive strength respectively, ε_c is strain, $\varepsilon_{c,o}$ is peak strain, \mathcal{V}_f is steel fiber volume fraction, and β is the factor which considers the fibers influence on the curve form.

This model is valid for concrete with compressive strength varying from 40 MPa to 60 MPa, produced with steel fibers 35 mm long and aspect ratio of 64 and with added steel fiber volumetric fractions of 1.0% and 2.0%.

In this study the adopted stress-strain curve in compression with compressive strength f'_c of 60 MPa, steel fiber volume fraction \mathcal{V}_f of 1% , fiber length L_f of 35 mm, and aspect ratio L_f/D_f of 64 is shown in Fig. 5.

- **Homogenization model for steel fiber in concrete in tension**

According to La Borderie in 1991 as cited by Pereira Junior, Araújo, and Pituba [17] the mechanical behavior of steel-fiber reinforced concrete structures subjected to loading and unloading processes depends mainly on the interaction between fibers and matrix. In this study, for the simulation of tensile behavior of the SFRC, the procedure of homogenization proposed by La Borderie is used. This proposed model was originally based on the homogenized stress-strain relationship introduced by Gilbert and Warner in 1978. The La Borderie established relationship of the steel fiber reinforced concrete in the governing tension regime is presented in Fig. 6, which is obtained from the fiber pullout test. The parameters that can be obtained from this test are peak stress (σ_{pic}), initial yield stress (σ_s), and ultimate strain (ε_{rupt}). It can be perceived that a simplifying assumption has been established: the strain of the matrix and fiber is considered the same. Moreover, the orientation of the random fiber is not taken into account in the proposed homogenization. However, this paper is not concerned with the exact values of these parameters, since the exact values can only be obtained from experimental tests, therefore an approximate prediction is sufficient based on some test works of earlier researchers in this field of flexural tensile strength of HS-SFRC with f'_c (60 MPa) and 1% \mathcal{V}_f steel fiber such as researchers' works in references [18] and [22].

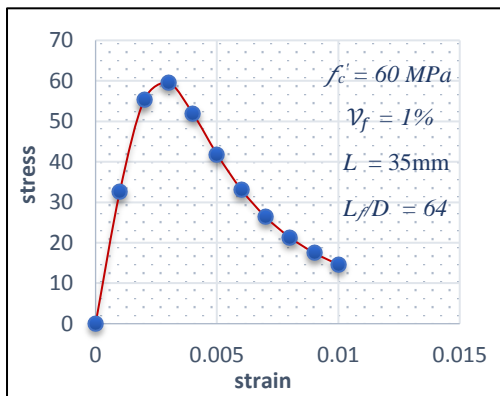


Fig. 5 - Analytical curve for HS-SFRC in compression used in this study

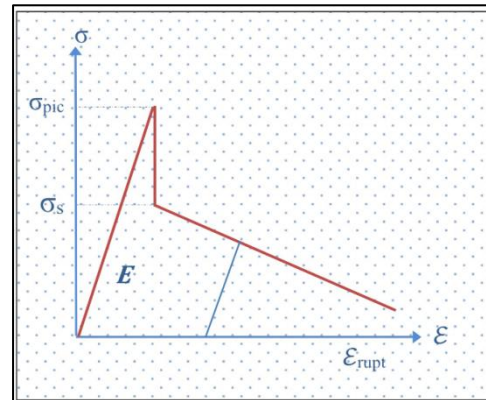


Fig. 6 - Model of tensile behavior in FRC proposed by La Borderie (1991) [17]

• **Modulus of elasticity and Poisson's ratio**

Modulus of elasticity E_c for HS-SFRC could be obtained by the same Eq. 4 introduced by ACI 363 for plain HSC, since it is confirmed that the addition of steel fiber has only a minor effect on the initial elastic modulus. However to be more specified the Eq. 5 is used in this study to estimate the value of E_c for HS-SFRC which is obtained from applying the regression analysis of many experimental data from Ashour, Wafa, and Kamal as cited by Abdul-Razzak, and Mohammed Ali [19].

$$E_c = 3,32\sqrt{f_c} + 6,9 \tag{4}$$

$$E_c = 3830\sqrt{f_{cf}} + 10^5 \nu_f \tag{5}$$

Where f_{cf} is the uniaxial compressive strength of HS-SFRC in MPa. Poisson's ratio ν for HS-SFRC was assumed as 0.2 in this study.

• **Plastic behavior of concrete**

Basically the required parameters to define the plasticity model of concrete are dilation angle ψ , the plastic potential eccentricity of concrete ϵ , the ratio of the biaxial compressive stress to the uniaxial compressive stress σ_{b0}/σ_{c0} , yielding surface shape factor in the deviatoric plane K_c , and viscosity parameter μ . For the concrete model to perform, only f_c and f_t need to be identified. Default values recommended by ABAQUS user manual [12] are assumed for the other five parameters.

For HS-SFRC, there is no information available from experimental tests to determine these parameters exactly. Holding high expectations for HSC with around 1% volume fraction of steel fiber to behave like concrete (isotropic material), the default values may then be sufficient approximation for the other five parameters, Table 2. However, there will always be probabilities of errors with these default values since there is no way to guarantee that the fibers are isotropically and uniformly packed in the entire concrete structure, also it is not possible to change the material model of concrete in ABAQUS so that the yield surface represents non-isotropic fiber efficiency.

Table 2 - Input parameters for plasticity section of CDP model

parameter	Default value
ψ	38°
ϵ	0.1
σ_{b0}/σ_{c0}	1.16
K_c	0.667
μ	0

4.2.2 Modeling of Reinforcing Bars

- **Steel bars**

In this study, to construct the reinforcement cage of the proposed specimens, deformed steel bars with diameter of 8 mm were used as stirrups and top bars (stirrup-holders) in compression zone.

For finite element model, the steel reinforcing bar is identical in both tension and compression and considered to be an elastic-perfectly plastic material. ABAQUS input data requirements for reinforcing steel are modulus of elasticity E_s , yield stress f_y , and Poisson’s ratio ν . The required material properties of the 8 mm steel stirrups and top bars used in this investigation are listed in Table 3. The yield stress f_y is obtained from a tensile test carried out at the university of Baghdad–consulting engineering bureau laboratories (CEBL)–metal lab, according to ASTM A 370 as shown in Fig. 9. The modulus of elasticity E_s and Poisson’s ratio ν for steel are assumed as 0.3 and 200 GPa respectively. Typical stress-strain relationship for steel reinforcing bar is shown in Fig. 7.

Table 3 – Material properties of steel stirrups and stirrup-holders

Diameter (mm)	Area (mm ²)	E_s (GPa)	f_y (MPa)	ϵ_y	ν
8	50.28	200	480	0.0024	0.3

- **FRP bars**

In this study two types of FRP rebars are considered as the main flexural reinforcement, glass fiber reinforced polymer (GFRP) with diameter of 12 mm and 10mm, and basalt fiber reinforced polymer (BFRP) rebars with diameter of 10mm and 6 mm. Fig. 10 shows the different types and diameters of the FRP rebar used in this study.

Glass fibers are the most commonly used fibers for producing FRP composites. However a basalt fiber (BFRP) has a high potential to provide satisfactory benefits that are comparable or superior to GFRP regarding the mechanical properties. Compared to glass fibers, basalt has higher tensile strength with considerably higher ultimate strain, and a modulus of elasticity that exceeds the elasticity of glass fibers [23].

In ABAQUS an isotropic linear elastic behavior was assumed for modeling the FRP bars, until failure without applying any damage criterion. This linear elastic behavior of FRP reinforced bars was assumed because of the brittle failure behavior they show after yielding without going to the plastic stage range [20] as shown in Fig. 8. The required proposed material properties of each type of FRP rebars are shown in Table 4 as provided by Hughes Brother, Inc.,USA., and Magmatech, company, UK., manufacturer for GFRP and BFRP respectively.

Table 4 - Material properties of glass and basalt FRP rebars used in this study

Manufacturer mechanical properties					
Rebar type	Nominal diameter (mm)	Modulus of elasticity (N/mm ²)	Rupture Stress (N/mm ²)	Rupture strain	Poisson’s ratio
	d	E_f	f_{fu}	ϵ_{fu}	ν
GFRP	10	40800	760	0.01862	0.25
GFRP	12	40800	690	0.01691	0.25
BFRP	10	50000	1000	0.0200	0.25
BFRP	6	50000	1000	0.0200	0.25

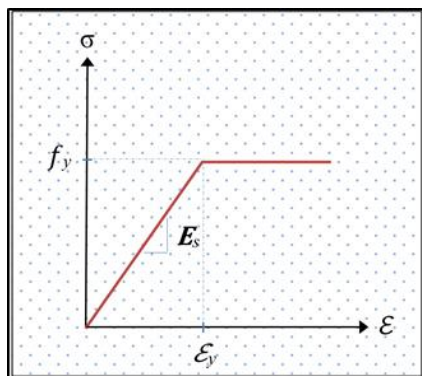


Fig. 7 - Typical stress-strain curve for steel reinforcing bar

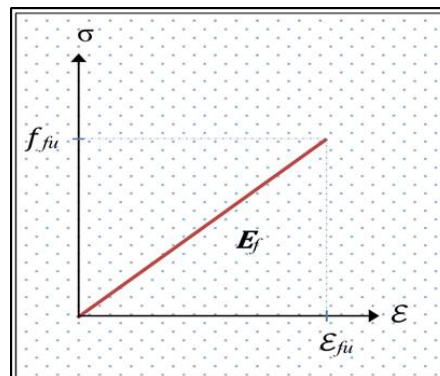


Fig. 8 - Typical linear elastic stress-strain behavior of FRP bars



Fig. 9 - The proposed 8 mm steel reinforcement tensile test at CEBL-Metal Lab

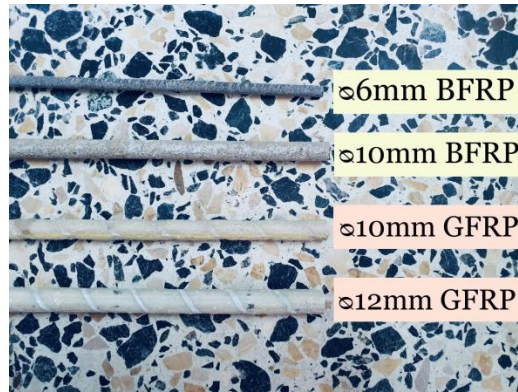


Fig. 10 - The proposed types and diameters of FRP rebar used in this study

5. FEA Results

5.1 General Behavior

The flexural behavior can be determined based on the ratio and type of reinforcement bars provided for the beam, as well as based on the shape and dimensions of the beam section. It is obvious from the test results in Table 5, that the different FRP reinforcement ratios and types and the beam cross section shape had some notable effects on the first cracking load and ultimate load capacity. However, on the other hand the shape of the beam cross-section exhibited rather significant influence on the ultimate load capacity, also it is worth mentioning that the deflection at mid span of all tested beams have not been affected remarkably by the considered variables in this study.

The first crack loads and ultimate load carrying capacities for all tested beams are shown in Fig. 11.

Table 5 - Test results of the proposed beams

Group design	Beam I.D.	Reinforcement ratio %	First crack		Peak state		Failure mode
		ρ_f^* %	P_{cr}^* (kN)	Δ_{cr}^* (mm)	P_u^* (kN)	Δ_u^* (mm)	
A	TG10	0.4787	48.4	0.46	78.5	1.32	C.C*
	TG12	0.6933	56.6	0.54	82.1	1.47	C.C
	TB10	0.4787	56.4	0.54	80.7	1.4	C.C
	TB6	0.1703	54.7	0.54	75.2	1.2	C.C
B	RG10	0.7180	41.7	0.57	57.8	1.3	C.C
	RB6	0.2555	41.3	0.57	55.5	1.2	C.C

Notes ; *C.C = Concrete crushing, * P_{cr} = First crack load, * Δ_{cr} = Mid span deflection at first crack load, * P_u = Ultimate load (peak load), * Δ_u = Mid span deflection at ultimate load,

$$* \rho_f = \frac{A_f}{A_{eff}} \quad (6)$$

- For rectangular cross-section $A_{eff} = b d$, see Fig. 17 - (a).
- For trapezoidal cross-section $A_{eff} = \frac{d}{2}(b_1 + b)$, see Fig. 17 - (b).

Where A_f is the area of FRP bars, and A_{eff} is the effective area of the beam cross-section.

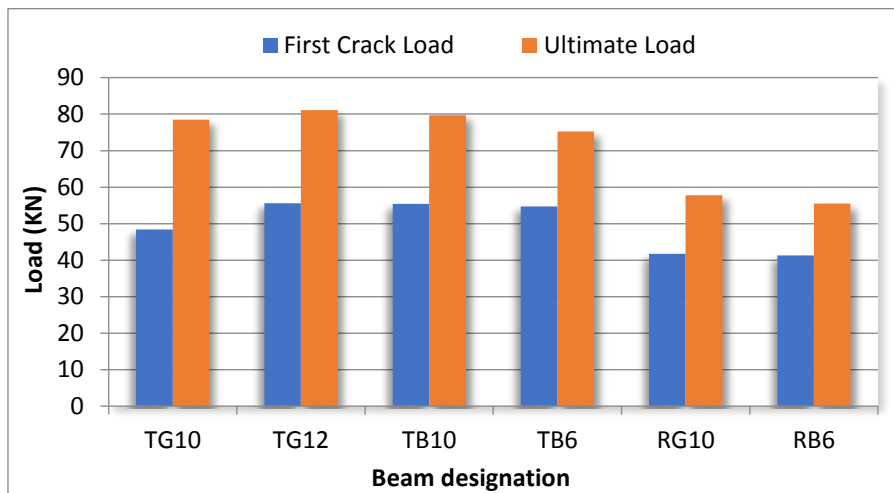


Fig. 11 - The load carrying capacity of all tested beams

5.2 Load-deflection Response

At the beginning before any observation of cracking, the relationship of load-deflection was identical and almost linear for all beams as it depends on the beam stiffness.

In general the load-deflection curve of plain FRP concrete beams keeps almost linear until failure, however the flexural stiffness significantly decreases quickly right away after the first crack formation due to the low elastic modulus of FRP rebars and inadequate tensile load carrying capacity of concrete [21–24]. Afterwards, the flexural stiffness gradually decreases with a steep increase in the cracks number and fast increase in crack width, and each beam behaves differently depending on the reinforcement type and ratio. Fig. 13 based on reference [24] depict such behavior of load-deflection of plain concrete reinforced with different types of FRP bars and the behavior of the curve is valid to be considered as a typical behavior regardless of the obtained data values that significantly differ from one research to another depending on many influential factors .

However, SFRC beams including FRP rebars exhibit a different behavior as shown in Fig. 12 in terms of showing a significant enhancement in flexural stiffness throughout the post-crack stage up to peak load, and showing a behavior of a gradual reduction (softening) in strength and higher residual strength in the post-peak stage, in other words behaving in a ductile way compared to conventional concrete beams. This behavior is attributed to steel fibers ability and role in bridging the cracks with their high elastic and shear modulus.

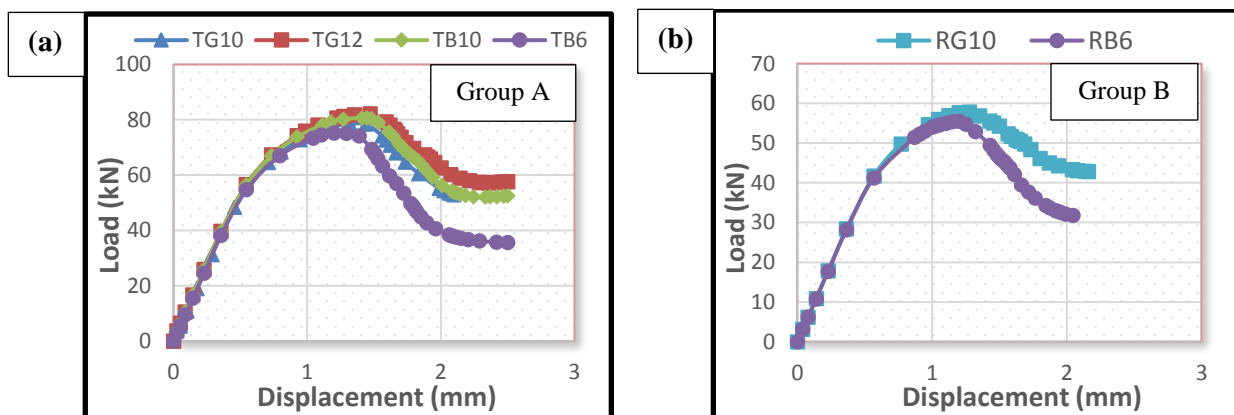


Fig. 12 - Load-deflection curves; (a) Group A; (b) Group B

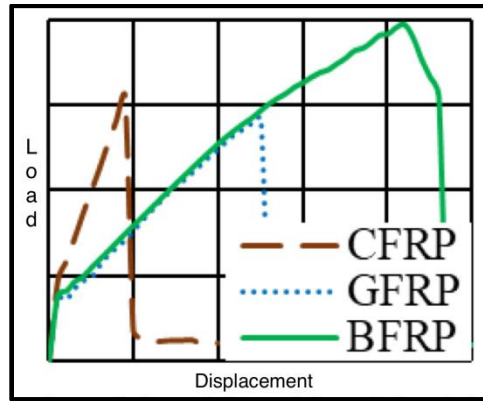


Fig. 13 - Typical load–deflection curve of conventional concrete beams reinforced with different types of FRP bar (carbon, glass, and basalt) FRP based on (Almeida Junior, Parvin) [24]

5.2.1 Effect of FRP Reinforcement Type

The load deflection response plotted in Fig. 14 shows that The behavior of the GFRP and BFRP reinforced beams are almost similar, however some improvement can be observed in the stiffness of the post cracking response of BFRP reinforced beam and an increase in the first crack load and ultimate load capacity of approximately 14.5% and 2.8% respectively with higher residual strength in the post-peak stage. These observed improvements are mostly owing to the higher Young’s modulus of the BFRP rebars and the higher rupture stress than the GFRP rebars.

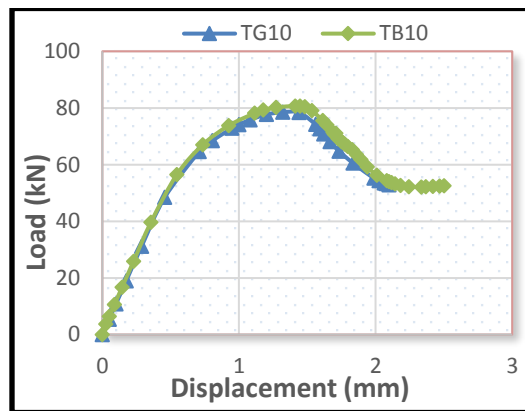


Fig. 14 - Load-deflection curves for beams TG10 and TB10

5.2.2 Effect of Reinforcement Ratio

It is obvious from Fig. 15 that higher GFRP and BFRP reinforcement ratios resulted in higher first cracking load and peak loads, which were found to be increased by 16.9% and 4.6% respectively, for 44.8% increase in GFRP reinforcement ratio, and by 3% and 7.3% respectively, for 181% increase in BFRP reinforcement ratio. For the higher reinforcement ratio a slightly stiffer post-cracking flexural behavior were observed. However the effect of increasing the reinforcement ratio manifested clearly on a more gradual reduction in strength and higher residual strength in post-peak stage for both cases of (a) and (b) in Fig 15.

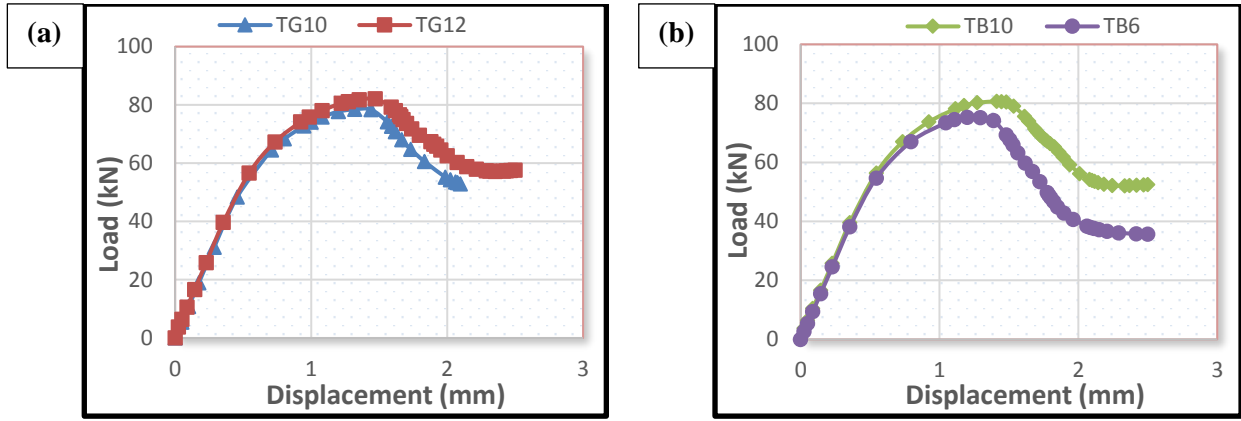


Fig. 15 - Load-deflection curves; (a) Beams TG10 and TG12; (b) Beams TB10 and TB6

5.2.3 Effect of Cross-section Shape

Fig. 16 shows the effects of top width of cross-section beams on their strength and load-deflection behavior. The results show that the trapezoidal cross section beams exhibited higher stiffness at post-cracking stage, which refer to a better fracture toughness, also the results indicate that the ultimate load capacity has increased by 35.5 to 35.8% when the top width of the beams increased from 125 mm to 250 mm, i.e. converting the beams from having a rectangular cross section to trapezoidal cross section. These improvements may be attributed to the compression area in the cross-section becoming bigger with any increase in the top width, causing the depth of the equivalent rectangular compression zone to be smaller, which lead to an increase in the moment arm from $(d - a/2)$ in rectangular cross-section case to $(d - y)$ in trapezoidal case (Fig. 17).

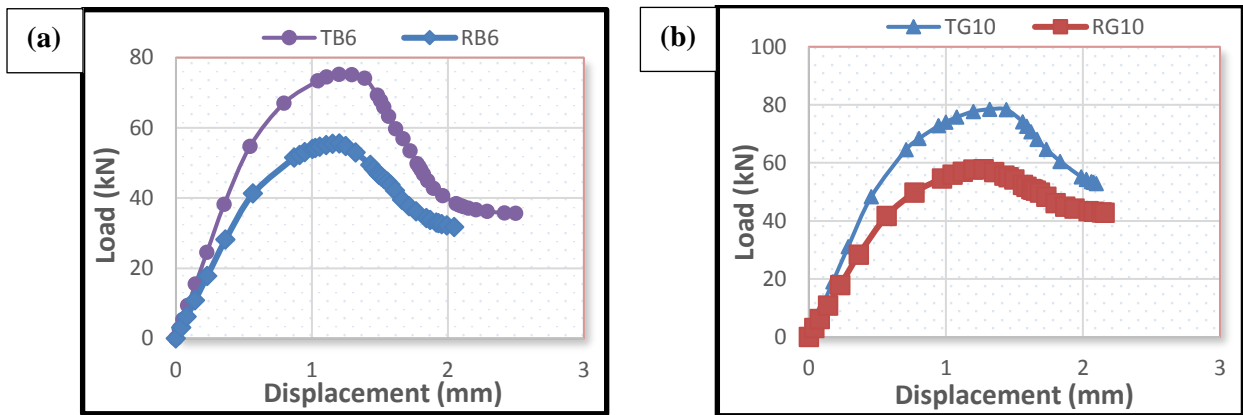


Fig. 16 - Load-deflection curves; (a) Beams TB6 and RB6; (b) Beams TG10 and RG10

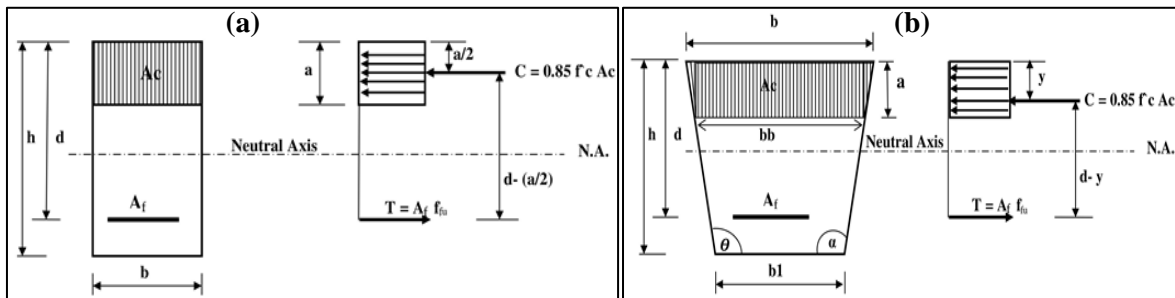


Fig. 17 - Equivalent rectangular flexural stress block distribution of singly FRP reinforced beam cross sections; (a) Rectangular cross-section beam; (b) Trapezoidal cross-section beam

5.3 Crack Patterns at Final Loading Stage

Cracks generated from initializing the stress field at the pure bending region by applying the two symmetrical point loads on each side of the test beams.

After reviewing cracking patterns of models at failure, which are shown in Fig. 18 it became clear that the cracks appear as a green region and initiate from the center then propagated upward toward the compression zone.

A major two facts reported from conducting this study are that all model beams were governed by concrete crushing failure mode with no widening of a flexural crack in the tension zones, also The cracks did not propagate rapidly in concrete beams due to combining the effects of HSC material, steel fiber, with FRP reinforcing bars regardless of whether the cross section of the beam is trapezoidal or rectangular.

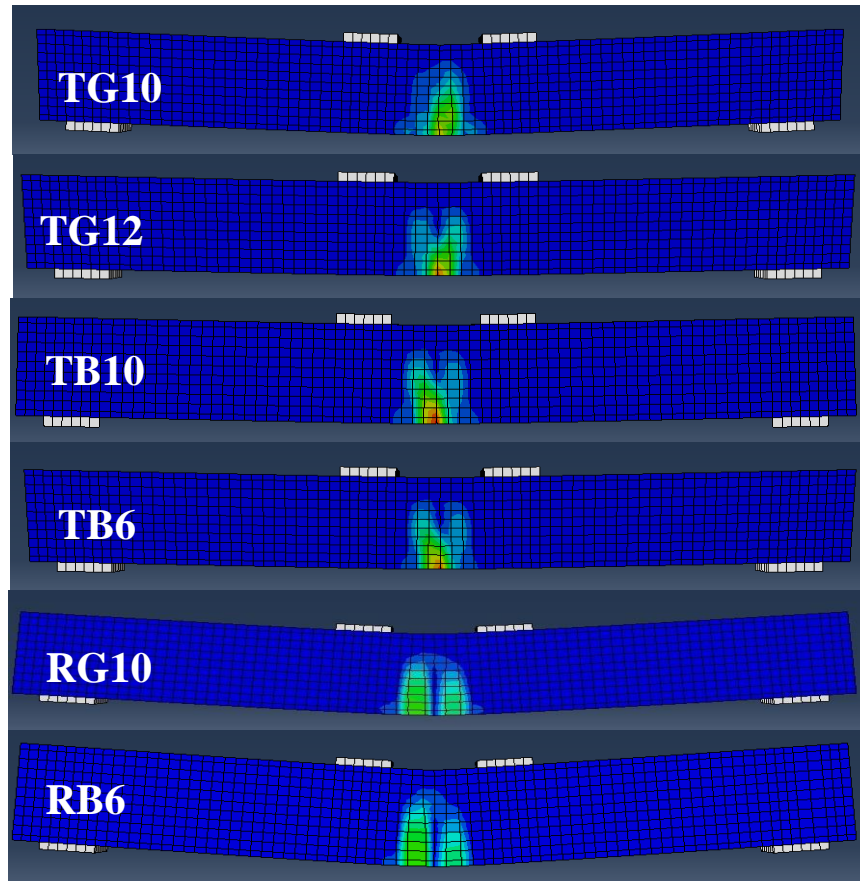


Fig. 18 - Crack patterns at failure of all beams models

6. Conclusions

In this study an investigation was performed by finite element analysis (FEA) by employing ABAQUS computer program incorporating the suggested material models. From the above discussions, the following conclusions were drawn.

1. The deflections were similar and were approximately 1.07–1.54 mm for all test beams. Because of its fiber bridging capacity on the crack surfaces, all the HS-SFRC beams exhibited stiff load–deflection curves at post-cracking stage and a gradual decrease in strength as well as a high residual strength in post- peak stage
2. When GFRP rebars replace by BFRP, the beam behaved almost similarly. However, an increase in the first crack load and ultimate load capacity of approximately 14.5% and 2.8% respectively were observed. The BFRP reinforced beam showed higher residual strength in the post- peak stage, also a slight improvement in the stiffness in the post cracking stage was noticed.
3. Higher post-cracking stiffness was observed with higher reinforcement ratio of FRP bars. The increases in the first crack load and ultimate load were found to be approximately 16.9 % and 4.6% respectively, for 44.8% increase in GFRP reinforcement ratio, and approximately 3% and 7.3% for 181% increase in the BFRP reinforcement ratio.

4. Converting the beam from having a rectangular cross section to trapezoidal by increasing the top width from 125 mm to 250 mm resulted in increasing the first crack load by 16 to 32.4%. The increase in ultimate load capacity was approximately 35.5 to 35.8% with higher post-cracking stiffness exhibition, which certainly refers to a better fracture toughness.
5. All test beams were governed by concrete crushing failure mode and the cracks did not propagate rapidly or deeply in concrete beams due to combining the effects of HSC material, steel fiber, and trapezoidal cross section with FRP rebars.

Acknowledgement

Many thanks to my supervisor Dr. Mushriq Fuad Kadhim Al-Shamaa (University of Baghdad) for his guidance and support throughout this research.

References

- [1] Ramadoss, P., & Nagamani, K. (2013). Stress-strain behavior and toughness of High-Performance Steel Fiber Reinforced Concrete in compression. *International Journal of Computers and Concrete*, Vol. 11, No. 2, pp. 149–167
- [2] Wang, H., & Belarbi, A. (2005). Flexural behavior of Fiber-Reinforced-Concrete beams reinforced with FRP rebars, 7th International Symposium on Fiber-Reinforced Polymer Reinforcement for Concrete Structures, SP-230, American Concrete Institute (ACI)
- [3] Belarbi, A., Chandraskhara, K., & Watkins, E.S. (1999). Performance evaluation of FRP rebar featuring ductility and health monitoring capability, 4th International Symposium on Fiber Reinforced Polymer Reinforcement for Reinforced Concrete Structures, SP-188, American Concrete Institute, Farmington Hills, Mich., pp.1–12
- [4] Harris, H. G., Somboonsong, W., & Frank, K. K. (1998). New ductile hybrid FRP reinforcement bar for concrete structures. *Journal of Composites for Construction*, ASCE, Vol. 2, No.1, pp. 28–37
- [5] Seongeun, K., & Seunghun, K. (2019). Flexural behavior of concrete beams with steel bar and FRP reinforcement. *Journal of Asian Architecture and Building Engineering*, Vol. 18, No. 2, pp. 89–97
- [6] Yinghao, L., & Yong, Y. (2013). Arrangement of hybrid rebars on flexural behavior of HSC beams. *Journal of Composites Part B: Engineering*, Vol. 45, No. 1, pp. 22–31
- [7] ACI Committee 440. (2015). Guide for the design and construction of concrete reinforced with FRP bars (ACI 440.1R-15). Farmington Hills, Mich: American Concrete Institute
- [8] Markovic, I. (2006). High performance hybrid fiber concrete: Development and utilization. PhD-thesis; TU Delft
- [9] Vandewalle, L. (2007). Postcracking behaviour of hybrid steel fiber reinforced concrete, in Proceedings of the 6th International Conference on Fracture Mechanics of Concrete and Concrete Structures, KU Leuven, pp. 1367–1376
- [10] Alsayed, H.S., & Alhozaimy, M. A. (1999). Ductility of concrete beams reinforced with FRP bars and steel fibers. *Journal of Composite Materials*, Vol. 33, No.19, pp. 1792–1806
- [11] Shafeeq, S., Al-Shathir, S. B., & Al-Hussnawi, M. (2018). Effects of trapezoidal cross-section dimensions on the behaviors of CFRP SCC beams, 2nd International Conference on Engineering Sciences: IOP Conference Series: Materials Science and Engineering, Vol. 433 012012
- [12] Smith, M. (2009). ABAQUS/Standard User's Manual, Version 6.14. Dassault Systems Simulia Corporation
- [13] Kodur, R. K. V., & Agrawal, A. (2016). An approach for evaluating residual capacity of reinforced concrete beams exposed to fire. *Engineering Structures journal*, Vol.110, pp. 293–306
- [14] Muhammad, H. J., & Abdulkadir, R. M. (2017). Nonlinear finite element modeling for high strength fibrous reinforced concrete beams. *Sulaimani Journal for Engineering Sciences*, Vol. 4, No. 4, pp. 14–28
- [15] Carreira, D. J., & Chu, K. H. (1985). Stress-strain relationship for plain concrete in compression. *ACI Journal*, Vol. 82, No. 6, pp. 797-804
- [16] Júnior, de O. Á. L. et al. (2010). Stress-strain curves for steel fiber-reinforced concrete in compression. *Revista Matéria*, Vol.15, No. 2, pp. 260–266
- [17] Pereira Junior, M. W., Araújo, D. L., & Pituba, C. J. J. (2016). Numerical analysis of steel-fiber-reinforced concrete beams using damage mechanics. *Ibracon Structures and Materials Journal*, Vol. 9, No. 2, pp. 153–191
- [18] Seok-Joon, J., et al. (2015). Feasibility of using high-performance steel fibre reinforced concrete for simplifying reinforcement details of critical members. *International Journal of Polymer Science*, Volume 2015, Article ID 850562
- [19] Abdul-Razzak, A. A., & Mohammed Ali, A. A. (2011). Modelling and numerical simulation of high strength fibre reinforced concrete corbels. *Applied Mathematical Modelling*, Vol. 35, pp. 2901–2915
- [20] Raza, A., Zaman Khan, uz Q., & Ahmad, A. (2019). Numerical investigation of load-carrying capacity of GFRP-reinforced rectangular concrete members using CDP model in ABAQUS. *Advances in Civil Engineering Journal*. Volume 2019, Article ID 1745341
- [21] Nanni, A. (1993). Flexural behavior and design of RC members using FRP reinforcement. *Journal of Structural Engineering (United States)*, Vol. 119, No. 11, pp. 3344–3359

- [22] Ramakrishnan, V., , Wu, G. Y., & Hosalli, G. (1989). Flexural behavior and toughness of fiber reinforced concretes, International symposium on recent developments in concrete fiber composites, Transportation Research Record. No. 1226, pp. 69 –77
- [23] Kampmann, R., Rambo-Roddenberry, M., & Telikapalli, S. (2019). Performance evaluation, material and specification development for basalt fiber reinforced polymer (BFRP) reinforcing bars embedded in concrete. Florida Department of Transportation, FSU Project, ID: 042088
- [24] Almeida Junior, A. S., & Parvin, A. (2019). Behavior of continuous concrete beams reinforced with basalt bars. SMAR 2019 – 5th Conference on Smart Monitoring, Assessment and Rehabilitation of Civil Structures, Interdependence between Structural Engineering and Construction Management